RESEARCH PAPER

The Effect of Sputtering RF Power on Structural, Optical and Electrical Properties of CuO and CuO$_2$ Thin Films

Alireza Razeghizadeh [1], Maryam Mahmoudi Ghalvandi [1], Farhang Sohilian [2], Vahdat Rafee [1,]*

[1] *Department of Physics, Faculty of Science, Payame Noor University, Tehran, Iran*

[2] *Department of Physics, Faculty of Science, Kharazmi University, Tehran, Iran*

ARTICLE INFO

ABSTRACT

In this paper, the RF power change effect on the structural, optical and electrical properties of CuO thin films prepared by RF reactive magnetron sputtering deposited on glass substrates are studied. At first, the thin films are prepared at 150, 280, 310 and 340W respectively. Then, the films are characterized by XRD, AFM, Uv-visible and four-point probe analysis respectively. The results show that the crystallite size and lattice constant of samples increased from about 20 nm to 59 nm and 4.15 to 4.51 respectively with an increase in RF power from 150 to 340W. The AFM and four-point analysis results show that the samples deposited at 150 and 340W have smooth surfaces and more surface electrical resistance than the samples deposited at 280 and 310W because the dominant phase of samples prepared at 150 and 340W are CuO$_2$ and 280 and 310 are CuO respectively. Also, the results indicate the energy band gap increased from about 2.25 to 2.52eV with an increase in RF power from 150 to 340W and the extinction coefficient of samples prepared at 150W is more than samples prepared at 340W in all of the wavelength.

How to cite this article

INTRODUCTION

Copper oxide one of the most semiconductors is studied so far. The conductivity of this matter is P-type and the CuO crystal lattice is monoclinic [1]. Most recently, the researchers have produced n-type conductivity of CuO with changing of experimental conditions [2].

The copper oxide because of its dark color is a photovoltaic matter with high absorption coefficient [3]. CuO is a suitable candidate for solar cell because gap energy of CuO is between 1.2-2.1 eV and CuO has a low electron affinity (3.2 eV) [4, 5]. The researchers in recent researches are trying to produce better solar cells with changing experimental conditions [6].

In recent decades, the researchers focused on the copper oxide because the copper oxide applications in the industry have increased also trying to determine its properties continues. These researches on the copper oxide are very interesting because electrical, physical and structural properties of CuO, make CuO thin films suitable for many applications such as gas sensor [7], heterogeneous catalysts [8], photochromic device [9], smart windows [10], Li- ion battery [11] and LED lamps [12], catalytic activity [13] and photosynthesis and Biological activities [14].

Also, the copper oxide is the best matter to see the Bose-Einstein condensation of excitons [15]. In addition to, the copper oxide is cheaper and more environmentally friendly for industrial application because it's non-toxic and abundant than another

* *Corresponding Author Email: v.rafee@gmail.com*

semiconductor such as GaAs and Si Also, it's more available than SnO$_2$ and In$_2$O$_3$ [16].

Many processes have been developed for synthesis the CuO Nanostructures, e.g. electrochemical deposition [17], DC reactive magnetron sputtering [18], RF reactive magnetron sputtering [19], vacuum annealing [6], pulsed laser deposition [20, 21], reactive chemical vapor deposition [22].

Among these methods the DC reactive magnetron sputtering method is very good technique for prepared thin films, because this method is very controllable and usable in deposition on the large area substrates. In this method physical properties of the samples are control by the deposition parameters such as the Oxygen partial pressure, substrate bias voltage and temperature, sputtering pressure and sputtering power.

These researchers have focused on this material in recent years and investigated structural, optical, electrical and thermal properties [6, 15, 19].

In this paper, we prepared the CuO thin films by RF reactive magnetron sputtering deposited on glass substrates at different RF power. Then, the structural, optical and electrical properties of these layers being studied by XRD, AFM, Uv-visible and four-point probe analysis.

MATERIALS AND METHODS

The CuO thin film is prepared as follow. At first, a pure 99.95% copper target with 101.6 mm diameter and 8 mm thickness is polished using soft sanding and cleaned by aston and ethanol. Then, the argon and oxygen gas is used as work gas sputtering process. Also, the glass substrates cleaned perfectly in aston and etanol solution using an ultrasonic cleaner. The experimental conditions except RF power sputtering are fixed for all of the four steps at during experiment.

The each step of the experiment is 1100 seconds. Any external heat does not apply to the system. Table 1 shows the details of the deposition process.

Then, the structural of samples are investigated using XRD analysis (XRD: Model D8 advance Bruker). Also, the morphology of samples is studied using AFM analysis (AFM: Model DME DS 95-50). The scan zone is 2×2 μm and the figure of AFM is tree dimensional.

In order to study of properties such as extinction coefficient, refractive index, energy gap, transmission spectrum and reflection spectrum are used for spectroscopy analysis. (Uv-visible: Model Gray 500scan). Finally, the surface electrical resistance of samples is studied by four point probe analysis (Four-point-probe: Model 196SYS DMM keithley).

RESULT AND DISCUSSION

Structural properties

XRD analysis

In order to study the structural properties of samples, the samples are considered using XRD at 2θ range equal 10 to 100 degree using Cu Kα radiation of wavelength λ=1.5406Å.

Fig. 1 shows that dominant phase of samples is changed of CuO to Cu$_2$O also the peaks of XRD are sharper with increasing RF power sputtering.

Usually the peaks are sharper because of increased grain size and clutter structural of samples [23, 24].

The crystallite size of samples are calculated using Debye-Scherrer equation as fallowing [25, 26]:

$$D = \frac{k\lambda}{\beta\cos\theta} \tag{1}$$

Where λ is the applied X-ray wavelength, θ the diffraction angle in degree and β is the full width at half maximum (FWHM) of the diffraction peak observed in radians. In order to study the lattice constant we used Bragg equation as fallowing [27]:

$$n\lambda = 2d\sin\theta \tag{2}$$

Where n is an integer number, θ the diffraction angle in degree and d is the spacing of lattice planes.

Table 1. Working conditions of RF reactive magnetic sputtering of deposition process

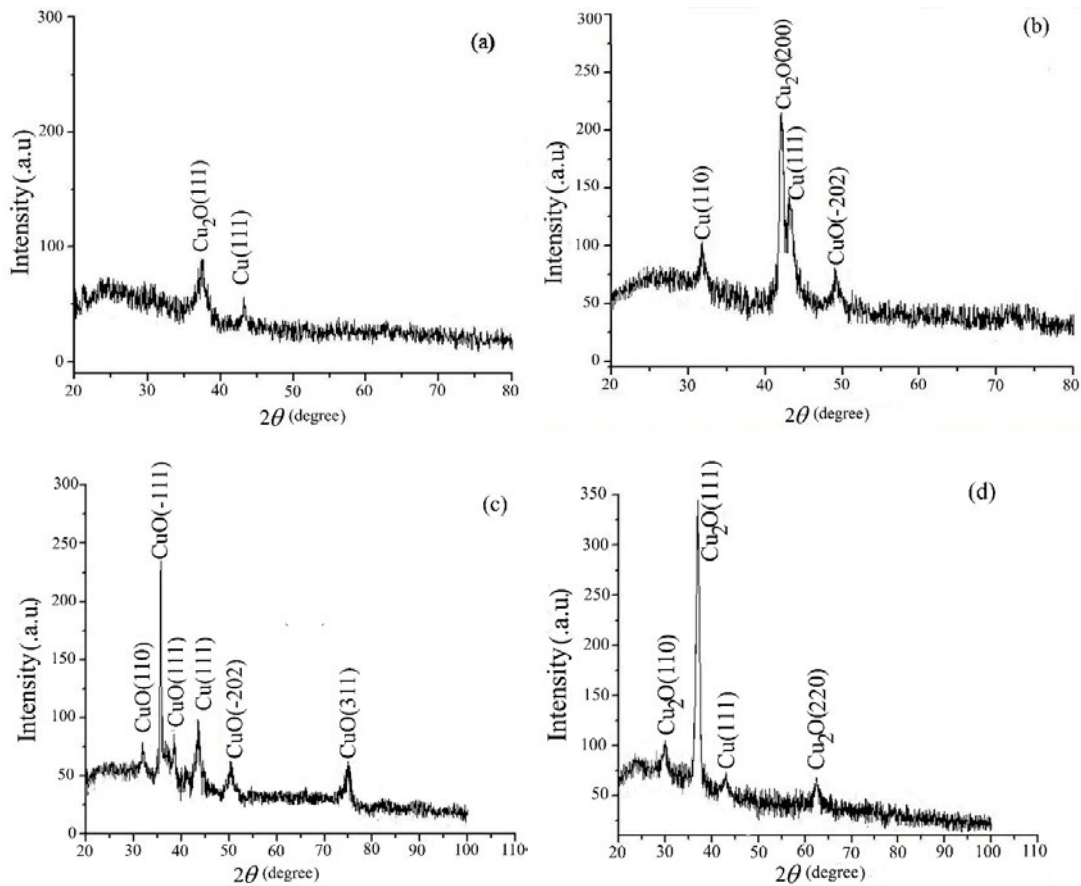| O pressure (mbar)	Ar pressure (mbar)	Returned power (W)	Input power (W)	Working pressure P(Ar+O$_2$) (mbar)
1×10^{-2}	2.45×10^{-2}	6	153	3.5×10^{-2}
1.1×10^{-2}	2.57×10^{-2}	8	282	3.6×10^{-2}
1×10^{-2}	2.49×10^{-2}	9	313	3.5×10^{-2}
1×10^{-2}	2.49×10^{-2}	9	343	3.5×10^{-2}

Fig. 1. XDR of the CuO thin films prepared at different RF power sputtering (a): 150 (W), (b): 280 (W), (c): 310 (W) and (d): 340 (W)

Table 2. The crystallite size and lattice constant of the CuO thin films prepared at different RF power sputtering

RF power sputtering (W)	crystallite size (nm)	lattice constant (Å)
150	20	4.15
280	28	4.28
310	44	4.49
340	59	4.51

Table 2 shows the result of the crystallite size and lattice constant of samples versus different the RF power sputtering. The results show that the average of the crystallite size of samples increases from 20nm to 59nm also and lattice constant increase from 4.15Å to 4.51Å with increasing of the RF sputtering power respectively.

AFM analysis

The morphology of samples are studied using AFM analysis at scan zone equal 2×2 μm and the figure of AFM is tree dimensional.

Fig. 2 shows the surface roughness of samples.

Fig. 2(a-d) shows different factor such as layer roughness, roughness height and surface area of samples are changed with increasing of RF power sputtering.

The results of AFM analysis shown in Table 3. So that, S_a, S_q, S_{tr}, S_{dq} and S_{dr} is the average watts roughness, the standard deviation (root mean square), the surface isotropy, the gradient of root mean square, and the percentage of surface area respectively. The results indicate that S_{dq}, S_{dr} is increased with increasing RF power sputtering. Finally, The AFM results show that the surface of samples with Cu_2O as dominant phase (The samples
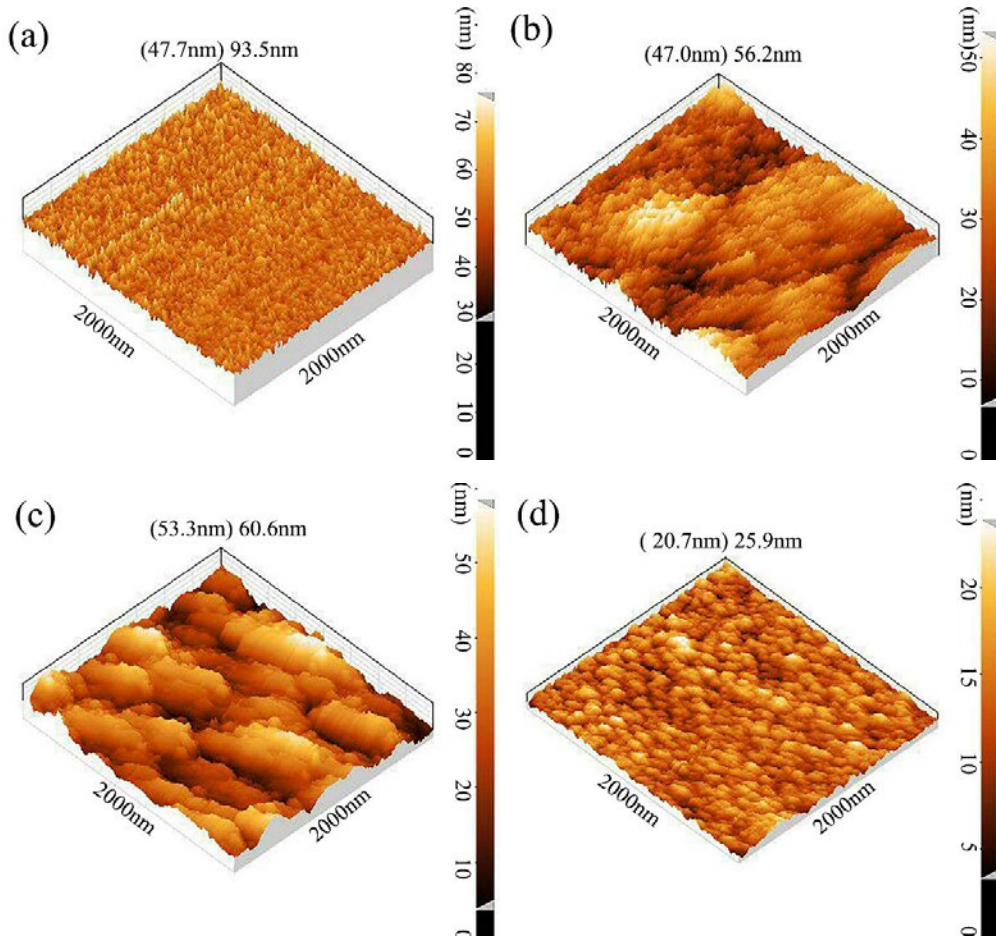
Fig. 2. 3D picture AFM of the CuO thin films prepared at different RF power sputtering (a): 150 (W), (b): 280 (W), (c): 310 (W) and (d): 340 (W)

Table 3. The AFM results of the CuO thin films prepared at different RF power sputtering

RF power sputtering (W)	S$_{dr}$	S$_{tr}$	S$_{dq}$	Sq (nm)	Sa (nm)
150	25.20%	0.49	0.75	6.17	4.63
280	6.67%	0.57	0.37	7.79	6.23
310	4.68%	0.37	0.31	9.94	8.02
340	2.75%	0.50	0.24	3.25	2.60

prepared at 150 and 340W) is smoother and also the surface of samples with CuO as dominant phase (The samples prepared at 280 and 310W) is sharper because these samples have more unreactive copper atoms. Therefore, the samples prepared at 280 and 310W exhibit more metallic behavior. Also, the hardness and light transmittance in these layers increase and decrease respectively.

Optical properties
Uv-visible analysis
Transmitting and reflecting spectrum

In order to study the optical properties of the samples such as transmittance rate, reflectance rate, optical energy gap, extinction coefficient, absorption coefficient and the refractive index of the layers the researchers used Uv-visible analysis.

Fig. 3 shows that the prepared samples at 280 and 310 W exhibit more metal since because these samples have more unreactive copper atoms, though produced samples at 150 and 340 W showed better semiconductor behavior. As a result, Fig. 3b shows that transmission spectrum of the layers deposited at 280 and 310 W equal to zero. This is another reason to prove that XRD and AFM sample results which mean the dominant phase of samples are CuO, also these have more hardness and more unreactive copper atoms. Also the results show that increase of power of deposited samples at 150 and 340 W cause a decrease of transmission percent in all wavelengths which is compatible with AFM results. Also, Fig. 3b shows that the transmission percent of the prepared sample at 340 W is less than the prepared sample at 150 W because the former has less surface roughness than later.

In the following, obtained a result from reflection spectrum in Fig. 3a shows that in both sample series which were produced at 280 and 310 W and samples at 150 and 340 W, reflection percent is decreased with the increase of power. This is completely expectable regarding increase size of gradation seen in AFM analysis. In the Table 2, results show that roughness increase with the increase of power from 150 to 310 that will display finer gradation. Only the sample at 340 W does not follow this pattern which is expectable considering the least amount of unreacted copper atom in the sample and the presence of Cu$_2$O phase and maximum semiconductor behavior of the sample.

Therefore, the AFM and UV-visible result present acceptable agreement.

Refractive index, extinction coefficient, absorption coefficient and Thickness

In 1983, Swanepol shows that the refractive index of layers with uniform thickness d, refractive index n, and absorption coefficient α and deposition on the substrate with refractive index equal n$_s$ can be calculated using maximum and minimum the transmittance spectrum T$_M$(λ), T$_m$(λ) respectively in the region of weak and medium absorption as follows [28]:

$$n = [N + (N^2 + n_s^2)^{\frac{1}{2}}]^{\frac{1}{2}} \qquad (3)$$

where n$_s$ is the refractive index of the substrate and also for glass equal 1.50 and N calculated as follows [28]:

$$N = 2n_s \frac{T_M - T_m}{T_M T_m} + \frac{n_s^2 + 1}{2} \qquad (4)$$

Where T$_M$ is a maximum envelope and T$_m$ is a minimum envelope. Estimating refraction coefficient of the layer according to two neighboring maximum (or two neighboring minimum), n$_1$ at point λ₁ and n$_2$ at the point λ₂, the layer thickness can be obtained by the following relation [28]:

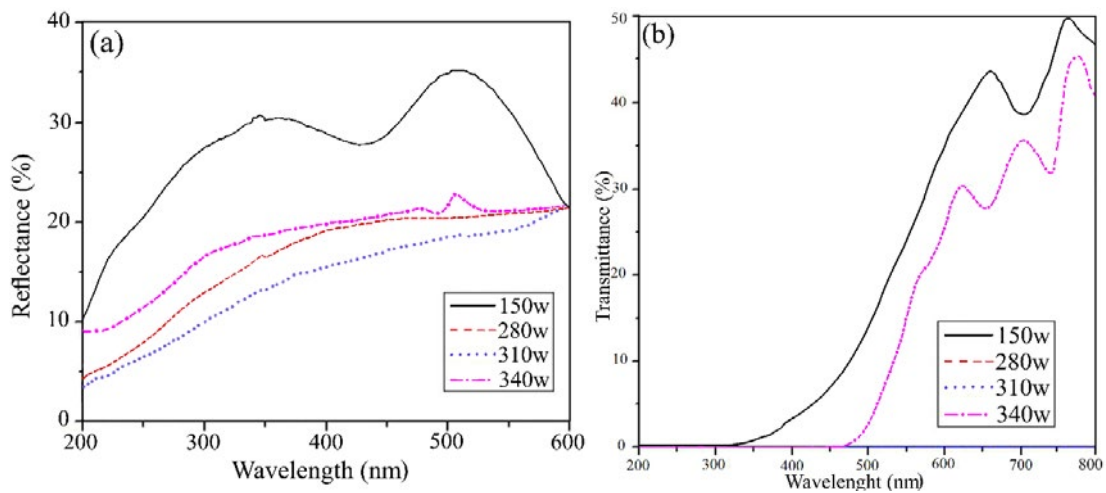$$d = \frac{\lambda_1 \lambda_2}{2(\lambda_1 n_2 - \lambda_2 n_1)} \qquad (5)$$

Fig. 3. Transmitting and reflecting spectrum of the CuO thin films prepared at different RF power sputtering (a) Reflecting spectrum, (b) Transmitting spectrum

The absorption coefficient can be obtained using thickness and refraction coefficient as fallows: [28]:

$$\alpha(\lambda) = -\frac{1}{d} \ln \left[\frac{(n-1)(n-n_s)\left(\frac{T_M}{T_m}+1\right)^{\frac{1}{2}}}{(n+1)(n+n_s)\left(\frac{T_M}{T_m}-1\right)^{\frac{1}{2}}} \right] \qquad (6)$$

Extinction coefficient also can be obtained using below relationship [28]:

$$k(\lambda) = \frac{\alpha(\lambda) \times \lambda}{4\pi} \qquad (7)$$

Table 4 shows the results related to thin layers of copper oxide deposited on glass substrate at 150 and 340 W. The results of prepared samples at 280 and 310 W are not considered in the estimation because these layers have more metal properties therefore transmission spectrums of these layers equal to zero.

The results of Table 4 show that the layer thickness, refraction and absorption coefficients of the layers prepared at 150 and 340 W totally increase with increasing power from 150 to 340 W because the dominant phase in these layers is a Cu$_2$O phase and these layers have better semiconductor properties. This result is completely consistence with the obtained conclusion in transmission spectrum which shows that increasing power cause decrease transmission percent and roughness of prepared layer at 340 W is less than that at 150 W in AFM analysis.

Fig. 4 also shows that power increase leads to decrease of extinction coefficient in all wavelengths.

Optical gap energy

With absorption coefficient α(λ) and Taus relationship, it can easily estimate optical energy gap of layers by using below equation [29]:

$$\alpha(\lambda) = \frac{A(h\nu - E_g)^{\frac{1}{2}}}{h\nu} \qquad (8)$$

Table 4. Refractive index, absorption coefficient and thickness of the CuO thin films prepared at different RF power

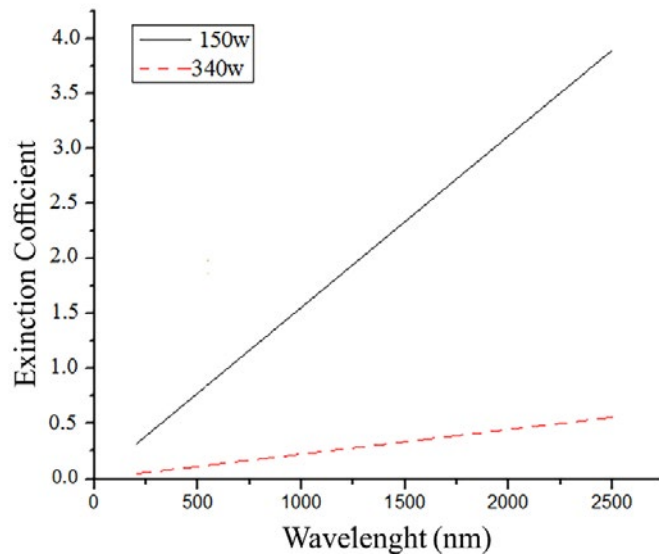| RF power sputtering (W)	Thickness (nm)	Refractive index	Absorption coefficient (nm⁻¹)
150	304.86	1.54	0.019
340	1378.07	1.59	0.002

Fig. 4. Extinction coefficient of the CuO thin films prepared at different RF power sputtering
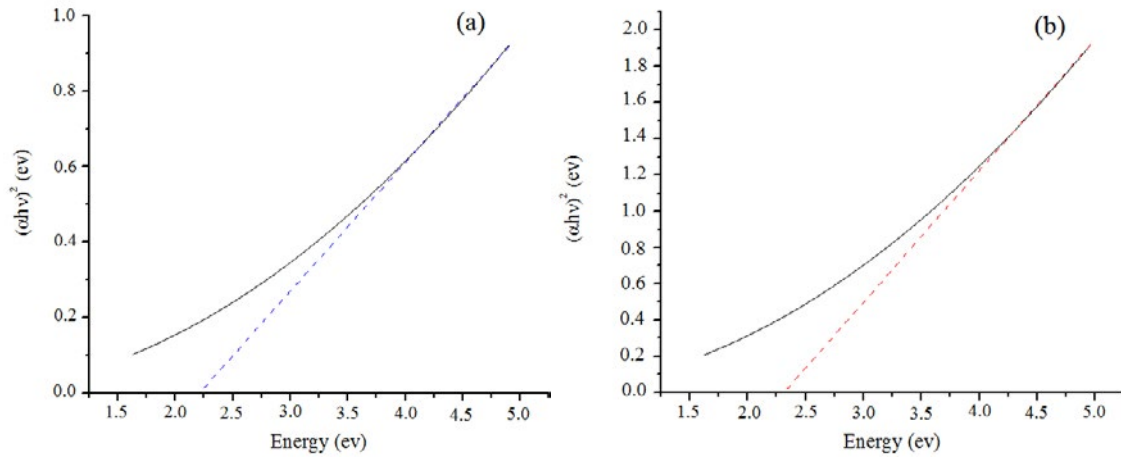
Fig. 5. Extinction coefficient of the CuO thin films prepared at different RF power sputtering (a) 150 (W), (b) 340 (W)

Table 5. The electrical properties of the CuO thin films prepared at different RF power

RF power sputtering (W)	Voltage (V)	Current (A)	Surface electrical resistance ($\Omega.cm$)
150	1.52	5×10^{-8}	1.35×10^{8}
280	0.45×10^{-3}	10^{-3}	2.00
310	1.7×10^{-3}	10^{-2}	0.76
340	4.0×10^{-3}	10^{-8}	17.95×10^{5}

Where, A is a constant value, h is Planck's constant and E$_g$ is energy gap.

Energy gap can be calculated by drawing the tangent line on the curve (αhv)^2 versus hv and obtaining intersection with energy axis α=0. As Fig. 5 shows, the optical energy gap of layers increases from 2.19 to 2.31 when power increase from 150 to 340.

Electrical properties
Surface electrical resistance
The surface electrical resistance of deposited samples is measured by the surface resistance measurement device by the four-point method. Measurement results are presented in Table 5. Results obtained from measuring the electrical resistance of deposited copper oxides layers on glass substrate show that deposited layers at 280 and 310 W have less resistance related to deposited layers at 340 and 150 W. Low resistance at 150 and 280 W can be due to the presence of unreacted copper atoms in the layers which are consistence with obtained results of Uv-visible and AFM. Also the results at 150 and 340 W series and 280 and 310 W series show that increase power leads to decrease of surface electrical resistance.

CONCLUSION
In this paper, we studied the RF power change effect on the structural, optical and electrical properties of CuO thin films prepared by RF reactive magnetron sputtering deposited on glass substrates.

The results indicate that the lattice constant, crystallite size and energy band gap of samples increased with an increase in RF power. Also, the results show that extinction coefficient of samples prepared at 150W is more than samples prepared at 340W in all of the wavelength.

The study of structural and electrical properties show that the samples deposited at 150 and 340W have smooth surfaces and more surface electrical resistance than the samples deposited at 280 and 310W because the dominant phase of samples prepared at 150 and 340W are CuO$_2$ and 280 and 310 are CuO respectively.

Finally, we find that deposited samples at 340 and 150 W show better semiconductor behavior but deposited samples at 280 and 310 W display more metal behavior.

CONFLICT OF INTEREST

The authors declare that there are no conflicts of interest regarding the publication of this manuscript.

REFERENCES

1. Hübner M, Simion CE, Tomescu-Stănoiu A, Pokhrel S, Bârsan N, Weimar U. Influence of humidity on CO sensing with p-type CuO thick film gas sensors. Sensors and Actuators B: Chemical. 2011;153(2):347-53.

2. Han K, Tao M. Electrochemically deposited p–n homojunction cuprous oxide solar cells. Solar Energy Materials and Solar Cells. 2009;93(1):153-7.

3. Li HJ, Pu CY, Ma CY, Li S, Dong WJ, Bao SY, et al. Growth behavior and optical properties of N-doped Cu2O films. Thin Solid Films. 2011;520(1):212-6.

4. Tolstova Y, Wilson SS, Atwater HA. Single phase, single orientation Cu 2 O (1 0 0) and (1 1 0) thin films grown by plasma-assisted molecular beam epitaxy. Journal of Crystal Growth. 2015;410:77-81.

5. Li J, Mei Z, Ye D, Liang H, Liu Y, Du X. Growth of single-crystalline Cu2O (111) film on ultrathin MgO modified α-Al2O3 (0001) substrate by molecular beam epitaxy. Journal of Crystal Growth. 2012;353(1):63-7.

6. Murali DS, Kumar S, Choudhary RJ, Wadikar AD, Jain MK, Subrahmanyam A. Synthesis of Cu2O from CuO thin films: Optical and electrical properties. AIP Advances. 2015;5(4):047143.

7. Mazhar ME, Faglia G, Comini E, Zappa D, Baratto C, Sberveglieri G. Kelvin probe as an effective tool to develop sensitive p-type CuO gas sensors. Sensors and Actuators B: Chemical. 2016;222:1257-63.

8. Chaudhary GR, Bansal P, Kaur N, Mehta SK. Recyclable CuO nanoparticles as heterogeneous catalysts for the synthesis of xanthenes under solvent free conditions. RSC Adv. 2014;4(90):49462-70.

9. Tripathi M, Chawla P. Optimization of semiconductor ns-TiO2-CuO admixed photoelectrode for photoelectrochemical solar cell in regard to hydrogen production. International Journal of Hydrogen Energy. 2016;41(19):7993-6.

[10]. Neshkovska R. Electrochromic copper (i) oxide thin film as a candidate for smart window. Acta Technica Corviniensis-Bulletin of Engineering. 2016; 9(2):49.

11. Subalakshmi P, Sivashanmugam A. CuO nano hexagons, an efficient energy storage material for Li- ion battery application. Journal of Alloys and Compounds. 2017;690:523-31.

12. Mahdizadeh F, Aber S. Treatment of textile wastewater under visible LED lamps using CuO/ZnO nanoparticles immobilized on scoria rocks. RSC Advances. 2015;5(92):75474-82.

[13]. Saghatforoush LA, Sanati S, Marandi G, Hasanzadeh M. Synthesis, characterization and catalytic activity of CuO nanostructures using Schiff base copper complexes as a precursor. J Nanostruct. 2013; 3(1):33-41.

[14]. Pansambal S, Deshmukh K, Savale A, Ghotekar S, Pardeshi O, Jain G, Aher Y, Pore D. Phytosynthesis and Biological Activities of Fluorescent CuO Nanoparticles Using Acanthospermum hispidum L. Extract. J Nanostruct. 2017 Jul 1;7(3):165-74.

15. Kavoulakis GM, Mysyrowicz A. Auger decay, spin exchange, and their connection to Bose-Einstein condensation of excitons inCu2O. Physical Review B. 2000;61(24):16619-22.

16. Liu J, Ke J, Li D, Sun H, Liang P, Duan X, et al. Oxygen Vacancies in Shape Controlled Cu2O/Reduced Graphene Oxide/In2O3 Hybrid for Promoted Photocatalytic Water Oxidation and Degradation of Environmental Pollutants. ACS Applied Materials & Interfaces. 2017;9(13):11678-88.

17. Jeun J-H, Kim D-H, Hong S-H. SnO2/CuO nano-hybrid foams synthesized by electrochemical deposition and their gas sensing properties. Materials Letters. 2013;105:58-61.

18. Murali DS, Subrahmanyam A. Synthesis of low resistive p type Cu4O3thin films by DC reactive magnetron sputtering and conversion of Cu4O3into CuO by laser irradiation. Journal of Physics D: Applied Physics. 2016;49(37):375102.

19. Elfadill NG, Hashim MR, Chahrour KM, Qaeed MA, Chunsheng W. The influence of oxygen pressure on the growth of CuO nanostructures prepared by RF reactive magnetron sputtering. Journal of Materials Science: Materials in Electronics. 2013;25(1):262-6.

20. Hu X, Gao F, Xiang Y, Wu H, Zheng X, Jiang J, et al. Influence of oxygen pressure on the structural and electrical properties of CuO thin films prepared by pulsed laser deposition. Materials Letters. 2016;176:282-4.

21. Yousuf AK. Substrate Temperature Effect on the Structure, Morphological and Optical Properties of CuO/Sapphire Thin Films Prepared by Pulsed Laser deposition. Ibn AL-Haitham Journal For Pure and Applied Science. 2017; 27(2):78-86.

22. Koh T, O'Hara E, Gordon MJ. Growth of nanostructured CuO thin films via microplasma-assisted, reactive chemical vapor deposition at high pressures. Journal of Crystal Growth. 2013;363:69-75.

23. Sahu P, De M, Zdujić M. Microstructural characterization of the evolved phases of ball-milled α-Fe2O3 powder in air and oxygen atmosphere by Rietveld analysis. Materials Chemistry and Physics. 2003;82(3):864-76.

24. Šepelák V, Steinike U, Uecker DC, Wißmann S, Becker KD. Structural Disorder in Mechanosynthesized Zinc Ferrite. Journal of Solid State Chemistry. 1998;135(1):52-8.

25. Razeghizadeh A, Mahmoudi Ghalvandi M, Sohillian F, Rafee V. The Effect of Substrate on Structural and Electrical Properties of Cu3N Thin Film by DC Reactive Magnetron Sputtering. Phys Chem Res. 2017; 5(3):497-504.

26. Rafee, v.; razeghizadeh, a.; Kazeminezhad, i.; Zalaghi, L., Growth and Optical Properties Investigation of Pure and Al-doped SnO2 Nanostructures by Sol-Gel Method. IRAN J CHEM CHEM ENG, 2017.

27. Lin J-J, Chen Y-M. Amphiphilic Properties of Poly(oxyalkylene) amine-Intercalated Smectite Aluminosilicates. Langmuir. 2004;20(10):4261-4.

28. Swanepoel R. Determination of the thickness and optical constants of amorphous silicon. Journal of Physics E: Scientific Instruments. 1983;16(12):1214-22.

29. Burns, G. "Solid State Physics Academic Press Inc." *New York* (1985).